ГЕОЛОГІЧНА ІНФОРМАТИКА

УДК 550.832+550.834
DOI: http://doi.org/10.17721/1728-2713.92.15

D. Malytskyy[1], Dr. Sci. (Phys.-Math.), Prof.
E-mail: dmalytskyy@gmail.com;
D. Mikesell[1,2], PhD, Prof,
E-mail: DylanMikesell@boisestate.edu;
[1]Carpathian Branch of Subbotin Institute of Geophysics, NAS of Ukraine,
3-b Naukova Str., Lviv, 79060, Ukraine;
[2]The Department of Geosciences at Boise State University,
1910 University Drive, Boise, Idaho, 83725 The USA

THE DETERMINATION OF SOURCE MECHANISMS OF SMALL EARTHQUAKES BY MOMENT TENSOR INVERSION

(Представлено членом редакційної колегії д-ром фіз.-мат. наук, проф. Б.П. Масловим)

A method is presented for moment tensor inversion of only direct P-waveforms registered at only one station and a limited number of stations. The method is based on an inversion approach described in where a version of the matrix method has been developed for calculation of direct P-waves in horizontally layered half-space from a point source represented by its moment tensor. We describe a procedure for retrieving the source mechanism of small earthquakes based on interactive inversion of seismograms and demonstrate its application to two local earthquakes in the Boise region. The moment tensor inversion of seismogram data in this study is based on a point source model. The process includes generation of synthetic seismograms using the matrix method for an elastic, horizontally-layered, medium. In the paper, a method is presented for moment tensor inversion of only direct P- waves, which are less sensitive to path effects than reflected and converted waves. This approach significantly improves the inversion method accuracy and reliability. A point-source approximation is considered, with known location and origin time. Based on forward modeling, a numerical technique is developed for the inversion of observed waveforms for time history of the components of moment tensor M(t), obtained by generalized inversion.

Keywords: seismic moment tensor, source mechanism, small earthquakes, matrix method.

Introduction. Earthquake source mechanisms are of prime importance in the monitoring of local, regional and global seismicity, because they reflect the stress pattern acting in the area under study and may help to map its tectonic structure. On a global scale, sources of information are large and moderate earthquakes that occur in active tectonic regions and are recorded by seismic stations worldwide. Techniques for analyzing these data are well established, that is, from first motion polarity readings analysis to waveform modelling of surface and long period body waves (*Langston and Helmberger, 1975; Given et al., 1982; Dziewonski and Woodhouse, 1983; Nabelek, 1984; Sipkin, 1986*). Advantages of such teleseismic studies included the availability of recording stations that cover the source region and the simplicity of waveforms and structures involved at low frequencies. At regional and local scales however, the scope for such studies is limited due to the limited number of recording stations and their spatial distribution. This leads to a problem in obtaining reliable source information from regions where the majority of earthquakes are small. As a result of the wide deployment of highly sensitive digital seismic instruments, high quality waveform data from small earthquakes can now be obtained from regional or local networks. However, data from such networks are not simple to analyze. Reasons for this include the influence of heterogeneous structure between the source and the recording station and the significant amount of high frequency energy in the signal.

In general, the observed seismograms contain information about the source, the path and the recording instrument. The practical problem is to isolate information about the source by correcting for the path and instrument effects. The effect of the instrument is easily removed because the instrumental response is known, on the other hand, isolating the path effect relies on the (assumed) linear relationship between the observed ground displacement and the seismic moment tensor density (*Gilbert, 1970; Stump and Johnson, 1977; Aki and Richards, 1980; Jost and Herrmann, 1989*). In practice, however, complete isolation of the path effect has proved difficult because a simple point source approach and flat layered structure model are not always good approximations, especially for high frequency data (*Lay and Wallace, 1995*). As propagation effects can never be fully excluded, they give rise to mislocation of the hypocenter and spurious source complexities. To address the above problem, various approaches have been developed based on moment tensor inversion in the time or frequency domain (*Saikia and Herrmann, 1985; Kim, 1987; Fan and Wallace, 1991; Koch, 1991, a; Arvidsson and Kulhanek, 1994; Arvidsson, 1996; Zhu and Helmberger, 1996; Shomali and Slunga, 2000; Singh et al., 2000*). These methods differ mainly in the nature of the problem that sets the a priori constraints. In trying to minimize the influence of the crustal structure, which is normally associated with a time-shift of the various phases in a seismogram, different segments of the seismogram, that is, *P*, *S*, Rayleigh , Love etc., have been modelled separately (*Zhao and Helmberger, 1994; Nabelek and Xia, 1995*). The advantage of this approach is that each phase is aligned using its onset time instead of the origin time. The various phase shifts obtained can then be used to correct for the crustal structure. Assuming that direct *P* and *S* phases from shallow events at close epicentral distances are less affected by crustal structure, Schurr and Nabelek (1999) managed to obtain mechanisms for the aftershock sequence of the 1993 Scotts Mills event. Apart from modelling different segments of seismograms mentioned above, simultaneous inversion of both the source and the structure has been applied on full trace high frequency data in weakly heterogeneous structure (*Sileny et al., 1992; Sileny and Psencik, 1995*). In this approach, both the hypocenter and the structure are allowed to vary in a limited sense in order to obtain the best fit between the observed and synthetic data. In areas of strong lateral heterogeneity the approach has been modified by the use of different source–receiver propagation structures that produce the best fit (*Mao et al., 1994; Sileny et al., 1996; Singh et al., 2000*).

Ferdinand and Arvidsson (2002) used an interactive inversion approach to demonstrate the retrieval of the source parameters of three small earthquakes and developed a modified model of structure along the propagation path. Due to significant variation of structure through out the Mbeya local network (*Camelbeeck and Iranga, 1996*), a single station approach was used. Using trial and error, the initial structure along the propagation path was modified to obtain the best fit between observed and synthetic data. The final single station solution was then used to generate synthetics for forward modelling of the seismograms at other stations where the event was recorded. Deviations between synthetics and observed data allowed them to deduce structural differences along the various propagation paths. Moment tensor inversion was carried out by minimizing the L2 norm of the difference between synthetic and observed displacement data under a deviatoric condition. Results for the three small earthquakes showed good agreement between single station and multistation source solutions.

Currently, moment tensors are calculated by several approaches: using amplitudes of seismic waves (*Vavrychuk and Kuhn, 2012; Godano et al., 2011*), S/P amplitude ratios (*Hardebeck and Shearer, 2003*), or full waveforms (*Mai et al., 2016; Weber, 2006, 2016*). The inversion of full waveforms is a widely used approach applicable on all scales: from small to large earthquakes.

In this study, a method is presented for moment tensor inversion of only direct P- and/or S-waves, which are less sensitive to path effects modelling than reflected and converted waves, which significantly improves the method' accuracy and reliability. Based on forward modeling, a numerical technique is developed for the inversion of observed waveforms for the components of the moment tensor ***M(t)***, obtained by generalized inversion. Addressing the problem of unavoidable inaccuracy of seismic waves modelling, we propose to invert only the direct P- and/or S-waves instead of the full field. An advantage of inverting only the direct waves consists in their much lesser distortion, if compared to reflected and converted waves, by inaccurate modelling of velocity contrasts. Thus, the direct waves, consequently, have a much less distorted imprint of the source. An advantage, in this connection, of choosing the matrix method for calculation of the wave field consists in its ability to analytically isolate only the direct waves from the full field.

Methodology. Our approach is limited to the far field approximation of a point source. Following Aki and Richards (1980), if a point source equivalent of the extended source is assumed, the *n*-th component of the ground displacement U_n at an arbitrary position *r* at time *t* can be expressed as

$$U_n(t) = G_{nk,j}(t) \otimes M_{kj}(t), \tag{1}$$

where $G_{nk,j}$ is the *j* th spatial derivative of the far-field elastodynamic Green's function $G_{nk}(r, x, t)$ for the Earth between the source and receiver; M_{kj} is the moment tensor at the hypocenter point *x* and $\otimes$ denotes temporal convolution. Assuming that all components of M_{kj} in (1) have the same time dependence, say *s*(*t*), (1) becomes

$$U_n(t) = M_{kj}(G_{nk,j}(t) \otimes s(t)), \tag{2}$$

where M_{kj} is now a set of constants and *s*(*t*) is the source time function. The intention is to use observed ground displacements U_n to infer properties of the source as characterized by M_{kj}.

A method, presented here, enables one to obtain the focal mechanism solution by inversion of waveforms recorded at only one station. The inversion scheme consists of two steps. First (forward modeling), propagation of seismic waves in vertically inhomogeneous media is considered and a version of matrix method for calculation of synthetic seismograms on the upper surface of the horizontally layered isotropic medium is developed. The point source is located inside a layer and is represented with seismic moment tensor. The displacements on the upper surface are presented in matrix form in the frequency and wave number domain, separately for the far-field and the near-field (Malytskyy, 2010, 2016; Malytskyy and Kozlovskyy, 2014; Malytskyy and D'Amico, 2015). Subsequently, only the far-field displacements are considered and the wave-field from only direct P- and S-waves is isolated with application of eigenvector analysis reducing the problem to system of linear equations (*Malytskyy, 2016*). Subsequently (inverse modeling), spectra of the moment tensor components are calculated using a solution of generalized inversion and transformed to time domain by applying the inverse Fourier transform.

1. Forward modelling. Assuming that the point source, represented by a symmetric moment tensor **M**(*t*), is located within a stack of solid, isotropic, homogeneous, perfectly elastic layers with horizontal and perfectly contacting interfaces, the layers characterized by thickness, density, and velocities of P- and S-waves, the following expressions have been obtained by Malytskyy (2010, 2016) in cylindrical coordinates for the displacements $u_z^{(0)}(t,r,\varphi)$, $u_r^{(0)}(t,r,\varphi)$ and $u_\varphi^{(0)}(t,r,\varphi)$ on the upper surface of the half-space at *z*=0:

$$\begin{pmatrix} u_z^{(0)} \\ u_r^{(0)} \end{pmatrix} = \sum_{i=1}^{3} \int_0^\infty k^2 \mathbf{I}_i L^{-1}\left[m_i \mathbf{g}_i\right] dk ,$$

$$u_\varphi^{(0)} = \sum_{i=5}^{6} \int_0^\infty k^2 J_i L^{-1}\left[m_i g_{\varphi i}\right] dk , \tag{3}$$

where

$$m_1 = M_{xz}\cos\varphi + M_{yz}\sin\varphi , \quad m_2 = M_{zz} ,$$

$$m_3 = \cos^2\varphi \cdot M_{xx} + \sin^2\varphi \cdot M_{yy} + \sin 2\varphi \cdot M_{xy} ,$$

$$m_4 = -\cos 2\varphi \cdot M_{xx} + \cos 2\varphi \cdot M_{yy} - 2\sin 2\varphi \cdot M_{xy} ,$$

$$m_5 = M_{yz}\cos\varphi - M_{xz}\sin\varphi , \tag{4}$$

$$m_6 = \sin 2\varphi \cdot M_{xx} - \sin 2\varphi \cdot M_{yy} - 2\cos 2\varphi \cdot M_{xy} ,$$

M_{xx}, M_{xy},…, M_{zz} are the Cartesian components of the moment tensor ***M(ω)*** representing the source located at *r*=0, axis *x* pointing North and *y* East; *φ* is the station's azimuth (Fig. 1); *k* is the horizontal wave number; functions $\mathbf{g}_i = (g_{zi}, g_{ri})^T$ and $g_{\varphi i}$ contain propagation effects between the source and the receiver (*Malytskyy, 2010, 2016*); $\mathbf{I}_1 = \begin{pmatrix} J_1 & 0 \\ 0 & J_0 \end{pmatrix}$, $\mathbf{I}_2 = \begin{pmatrix} J_0 & 0 \\ 0 & J_1 \end{pmatrix}$, $\mathbf{I}_3 = \mathbf{I}_2$, $J_5 = J_0$, $J_6 = J_1$ are the Bessel functions of argument *kr*, and L^{-1} is the inverse Laplace transform, from frequency to time domain.

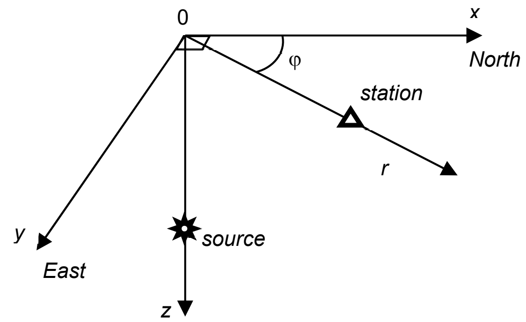

Fig. 1. Cylindrical and Cartesian coordinates of the source and the station

Further, only the far-field displacements are considered and the wave-field from only direct P- and S-waves is isolated with application of eigenvector analysis reducing the problem to system of linear equations (*Malytskyy, 2016*). The Eq. (3) is then expressed in matrix form for only the direct P- and S-waves on the upper surface of the half-space in frequency and wave number domain (ω, *k*) (*Malytskyy, 2010*):

$$\mathbf{U}^{(0)} = \mathbf{K} \cdot \boldsymbol{M} , \tag{5}$$

where vector $\mathbf{U}^{(0)} = \left(U_x^{(0)P}, U_x^{(0)S}, U_y^{(0)P}, U_y^{(0)S}, U_z^{(0)P}, U_z^{(0)S}\right)^T$ contains the six Cartesian displacement components of direct P- and *S*-waves; vector $\mathbf{M} = \left(M_{xz}, M_{yz}, M_{zz}, M_{xx}, M_{yy}, M_{xy}\right)^T$ consists of the six independent Cartesian components of moment tensor **M**, matrix **K** accounting for path effects and transformations between the Cartesian and cylindrical coordinates:

$$\mathbf{K} = \begin{pmatrix} K_{11}^P & K_{12}^P & K_{13}^P & K_{14}^P & K_{15}^P & K_{16}^P \\ K_{21}^S & K_{22}^S & K_{23}^S & K_{24}^S & K_{25}^S & K_{26}^S \\ K_{31}^P & K_{32}^P & K_{33}^P & K_{34}^P & K_{35}^P & K_{36}^P \\ K_{41}^S & K_{42}^S & K_{43}^S & K_{44}^S & K_{45}^S & K_{46}^S \\ K_{51}^P & K_{52}^P & K_{53}^P & K_{54}^P & K_{55}^P & K_{56}^P \\ K_{61}^S & K_{62}^S & K_{63}^S & K_{64}^S & K_{65}^S & K_{66}^S \end{pmatrix}.$$

When only the direct P-waves are used, matrix **K** reduces to

$$\mathbf{K}^P = \begin{pmatrix} K_{11}^P & K_{12}^P & K_{13}^P & K_{14}^P & K_{15}^P & K_{16}^P \\ K_{21}^P & K_{22}^P & K_{23}^P & K_{24}^P & K_{25}^P & K_{26}^P \\ K_{31}^P & K_{32}^P & K_{33}^P & K_{34}^P & K_{35}^P & K_{36}^P \end{pmatrix}.$$

Thus, the Eq. (5) can be written only for the direct P-waves in the matrix form:

$$\mathbf{U}^{(0)P} = \mathbf{K}^P \cdot \boldsymbol{M}, \qquad (6)$$

where $\mathbf{U}^{(0)P} = \left(U_x^{(0)P}, U_y^{(0)P}, U_z^{(0)P}\right)^T$ defines the observed amplitudes of the direct *P*-waves, and the components of matrix $\mathbf{K}^P$ are

$$K_{11}^P = \cos^2\varphi \cdot \int_0^\infty \frac{k^2 J_0(kr)}{2\pi j} g_{r1}^P\, dk,$$

$$K_{12}^P = \cos\varphi \sin\varphi \cdot \int_0^\infty \frac{k^2 J_0(kr)}{2\pi j} g_{r1}^P dk,$$

$$K_{13}^P = \cos\varphi \cdot \int_0^\infty \frac{k^2 J_1(kr)}{2\pi j} g_{r2}^P\, dk,$$

$$K_{14}^P = \cos^3\varphi \cdot \int_0^\infty \frac{k^2 J_1(kr)}{2\pi j} g_{r3}^P\, dk,$$

$$K_{15}^P = \cos\varphi \sin^2\varphi \cdot \int_0^\infty \frac{k^2 J_1(kr)}{2\pi j} g_{r3}^P\, dk,$$

$$K_{16}^P = \cos\varphi \sin 2\varphi \cdot \int_0^\infty \frac{k^2 J_1(kr)}{2\pi j} g_{r3}^P\, dk,$$

$$K_{21}^P = \sin\varphi \cos\varphi \cdot \int_0^\infty \frac{k^2 J_0(kr)}{2\pi j} g_{r1}^P dk,$$

$$K_{22}^P = \sin^2\varphi \cdot \int_0^\infty \frac{k^2 J_0(kr)}{2\pi j} g_{r1}^P dk,$$

$$K_{23}^P = \sin\varphi \cdot \int_0^\infty \frac{k^2 J_1(kr)}{2\pi j} g_{r2}^P dk,$$

$$K_{24}^P = \cos^2\varphi \sin\varphi \cdot \int_0^\infty \frac{k^2 J_1(kr)}{2\pi j} g_{r3}^P dk,$$

$$K_{25}^P = \sin^3\varphi \cdot \int_0^\infty \frac{k^2 J_1(kr)}{2\pi j} g_{r3}^P dk,$$

$$K_{26}^P = \sin\varphi \sin 2\varphi \cdot \int_0^\infty \frac{k^2 J_1(kr)}{2\pi j} g_{r3}^P dk,$$

$$K_{31}^P = \cos\varphi \cdot \int_0^\infty \frac{k^2 J_1(kr)}{2\pi j} g_{z1}^P\, dk,$$

$$K_{32}^P = \sin\varphi \cdot \int_0^\infty \frac{k^2 J_1(kr)}{2\pi j} g_{z1}^P\, dk,$$

$$K_{33}^P = \int_0^\infty \frac{k^2 J_0(kr)}{2\pi j} g_{z2}^P\, dk,$$

$$K_{34}^P = \cos^2\varphi \cdot \int_0^\infty \frac{k^2 J_0(kr)}{2\pi j} g_{r3}^P\, dk,$$

$$K_{35}^P = \sin^2\varphi \cdot \int_0^\infty \frac{k^2 J_0(kr)}{2\pi j} g_{r3}^P\, dk,$$

$$K_{36}^P = \sin 2\varphi \cdot \int_0^\infty \frac{k^2 J_0(kr)}{2\pi j} g_{z3}^P\, dk.$$

2. Inversion modeling. Now, that a direct relation between the moment tensor and the displacements on the free surface of the half-space is defined by Eq. (6), the moment tensor can be determined from the displacements by inverting the relation.

A least-squares solution to the over-determined system of Eq. (6) for $\boldsymbol{M}$ (for there are 3 × *k* × ω equations in total for 6 × ω unknowns) can be obtained by generalized inversion (*Aki and Richards, 2002*):

$$\boldsymbol{M} = (\tilde{\mathbf{K}}^P \mathbf{K}^P)^{-1} \tilde{\mathbf{K}}^P \mathbf{U}^{(0)P}, \qquad (7)$$

where the tilda denotes complex conjugation and transposition, and -1 inversion and $(\tilde{\mathbf{K}}^P \mathbf{K}^P)^{-1} \tilde{\mathbf{K}}^P$ is the generalized inverse of $\mathbf{K}^P$.

Thus, since all the six independent components of moment tensor $\boldsymbol{M}$ contribute to the waveforms $\boldsymbol{U}^{(0)}$ at only one station in the over-determined system of Eq. 6, the inversion scheme of Eq. 7 should enable, at least theoretically, to obtain a unique solution for each of them. Within the limitations of the current source presentation and path effects modeling, the solution is exact and convergence is reached after a single iteration. The inverse problem in this case consists of determining the parameters of point source under the condition that the source location and origin time is known, as well as the distribution of velocities of seismic waves between the source and the station.

Eq. (6) can be expressed in matrix form for direct P-waves at N stations (i = 1,…,N) in the spectral domain:

$$\boldsymbol{GM} = \boldsymbol{U}_{\boldsymbol{n}}^{(\mathbf{0})p}$$

$$\boldsymbol{G} = \begin{pmatrix} \boldsymbol{K}_1 \\ \vdots \\ \boldsymbol{K}_N \end{pmatrix},$$

$$\boldsymbol{U}_{\boldsymbol{n}}^{(\mathbf{0})p} = (\boldsymbol{U}_1^{(\mathbf{0})p}, \boldsymbol{U}_2^{(\mathbf{0})p}, \ldots, \boldsymbol{U}_N^{(\mathbf{0})p})^T$$

The vector $\boldsymbol{M}$ of moment time functions is obtained using the generalized inversion.

$$\widehat{\boldsymbol{M}} = (\widetilde{\boldsymbol{G}}^* \boldsymbol{G})^{-1} \widetilde{\boldsymbol{G}}^* \boldsymbol{U}_{\boldsymbol{n}}^{(\mathbf{0})p}$$

Application. In this section, the proposed inversion method is tested by applying it to two earthquakes from the Southeast Idaho region in the USA: one of them (event 1) has a known focal mechanism and the second (event 2) – has a unknown focal mechanism. 1D crustal model used in all the inversions of waveforms is listed in Table 1. The duration of direct P-waves at a station is estimated visually from the records, and accounting for the delays of reflection-conversion phases at the station corresponding to the model

(Table 1) at a respective epicentral distance and source depth (*Pang et al., 2018*).

Table 1

1D crustal model used in this study (*Shemeta, 1989*)

Depth, km	Velocity V_p, km/s	Velocity V_s, km/s
0.0	4.75	2.73
2.74	5.72	3.31
8.85	6.06	3.57
19.10	6.80	3.89
41.10	8.00	4.57

Fig. 2 shows the observed seismograms for the event 1 at stations AHID (42.77N, –111.10E) and IMW (43.89N, –110.94E) and for the event 2 at stations HLID (42.56N, –114.41E) and MFID (43.42N, –115.83E). Table 2 gives location parameters and magnitudes of these events. The components of moment tensor ***M(t)*** were obtained for the earthquake of 2017/09/02 (event 1) by inverting its direct P-wave forms at only the station AHID (at epicentral distance of 32 km) (Fig. 3, a) and at only at the stations: AHID (at epicentral distance of 32 km) and IMW (at epicentral distance of 144 km) (Fig. 3, b). The components of moment tensor ***M(t)*** were obtained for the earthquake of 2019/05/16 (event 2) by inverting its direct P-wave forms at only the stations: HLID (at epicentral distance of 114 km) and MFID (at epicentral distance of 178 km).

Table 2

Events used in this study

Event number	Date	Latitude	Longitude	Depth (km)	Magnitude	Origin time (UTC)
1	2017/09/02	42.65˚N	–111.45˚E	9.50	MW5.3	23:56:52.00
2	2019/05/16	44.578˚N	–114.298˚E	6.91	ML2.4	09:08:57.00

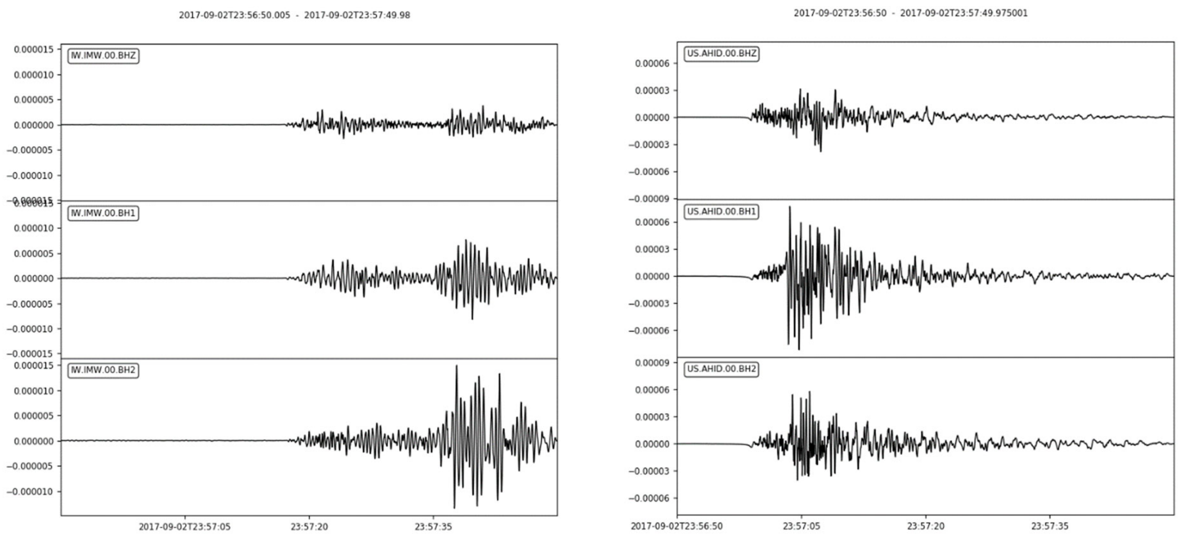

a

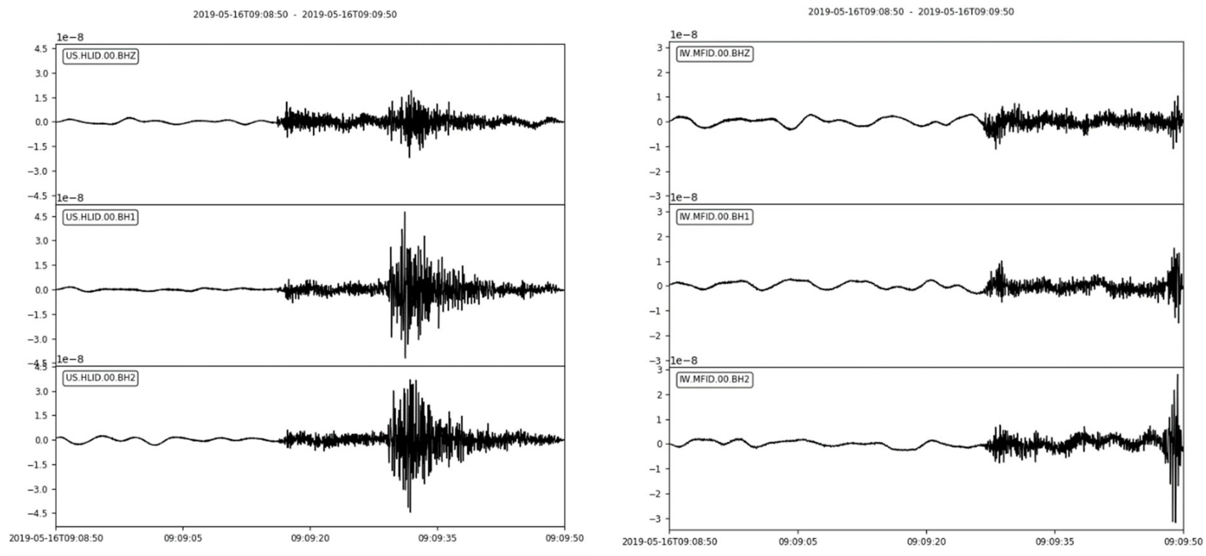

b

Fig. 2. a – The waveforms (seismograms) recorded at stations AHID (42.77N, –111.10E) and IMW (43.89N, –110.94E) (https://earthquake.usgs.gov/earthquakes/eventpage/us2000aekg/executive, event 1) after transform to displacements; b – The waveforms (seismograms) recorded at stations HLID (42.56N, –114.41E) and MFID (43.42N, –115.83E) (https://earthquake.usgs.gov/earthquakes/eventpage/mb80344114/executive, event 2) after transform to displacements. These records were used for a determination of seismic tensor by inversions of waveforms (see Fig. 3 and Fig. 5) using direct P-waves

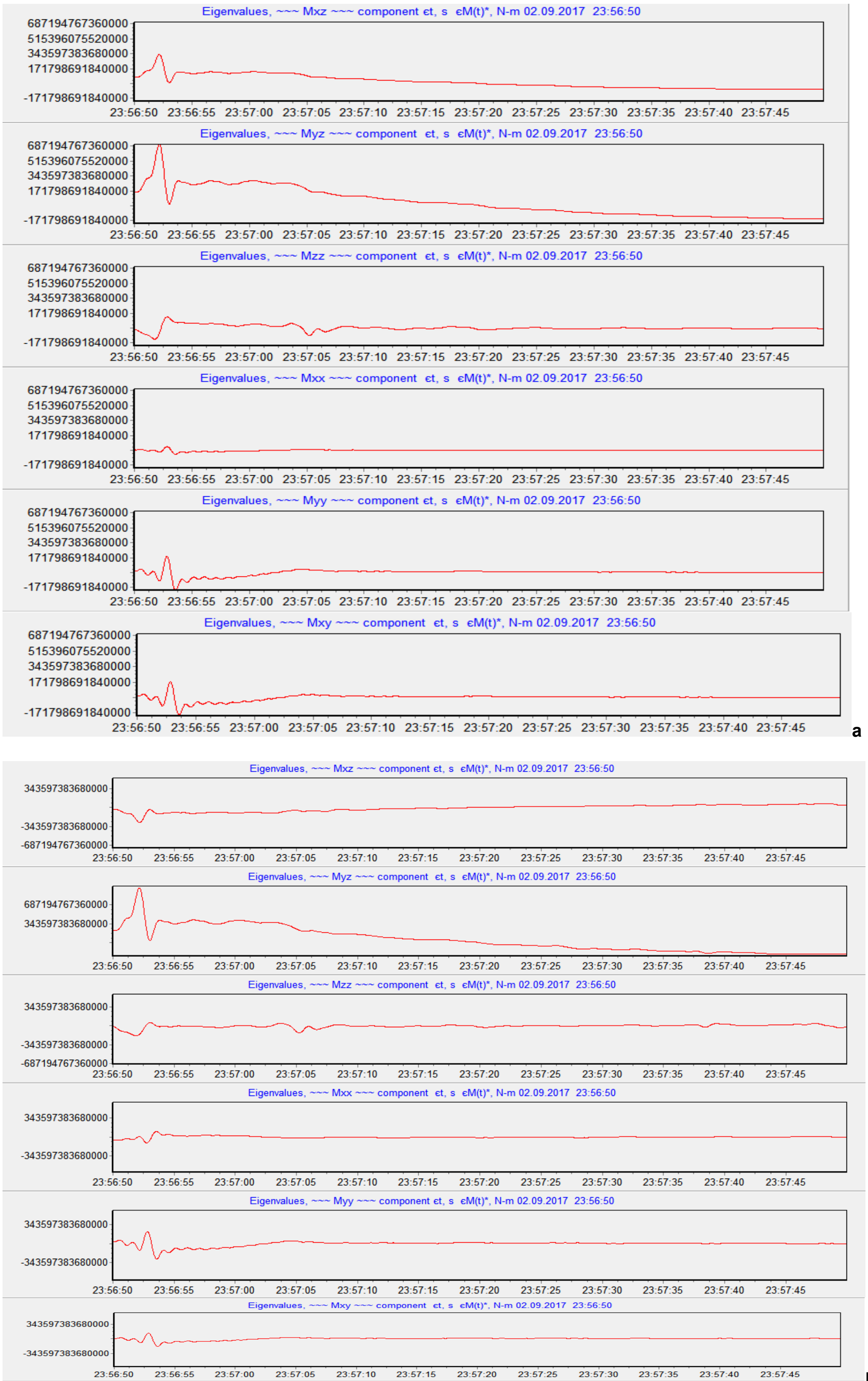

a

b

Fig. 3. a – components of moment tensor *M(t)* obtained for the earthquake of 2017/09/02 (event 1) in the Idaho region by inversion of its direct P-wave forms only at the station AHID; b – at the stations AHID and IMW

Moment tensor components resulting from the inversion of only direct P-wave forms at only the station AHID (Fig. 3, a) and the inversion of only direct P-wave forms at the stations AHID and IMW (Fig. 3, b) and the corresponding versions of focal mechanism for the event 1 are shown in Fig. 4.

Moment tensor components resulting from the inversion of only direct P-wave forms at the stations HLID and MFID (Fig. 5) and the corresponding version of focal mechanism for the event 2 are shown in Fig. 6.

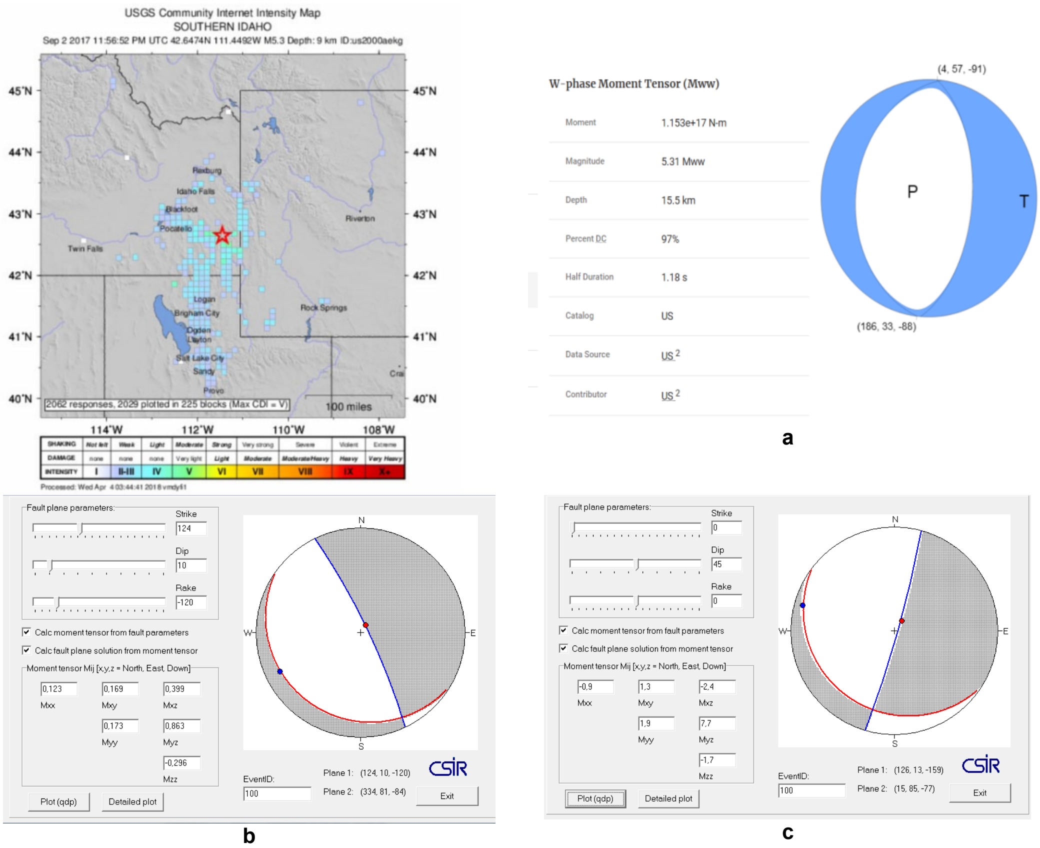

Fig. 4. Versions of focal mechanism for the earthquake that occurred on 2017/09/02 in the Idaho region (t_0 = 23:56:52.00 (UTC), h_s = 9.50 km, φ = 42.65˚N, λ = –111.45˚E, Mw = 5.3):
a – from https://earthquake.usgs.gov/earthquakes/eventpage/us2000aekg/executive;
b – corresponding to components of seismic tensor obtained by the proposed inversion of waveforms at only station AHID (42.77N, –111.10E) (see Fig. 3, a); c – corresponding to components of seismic tensor obtained by the proposed inversion of waveforms at stations: AHID (42.77N, –111.10E) and IMW (43.89N, –110.94E) (see Fig. 3, b)

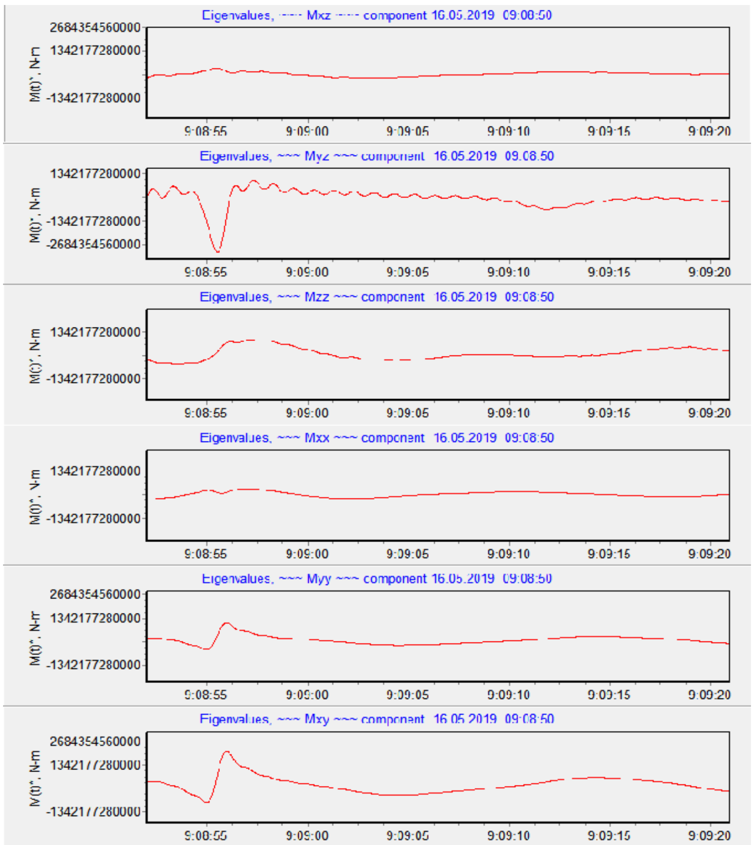

Fig. 5. Components of moment tensor *M(t)* obtained for the earthquake of 2019/05/16 in the Western Idaho region (event 2) by inversion of direct P-wave forms at the stations HLID and MFID

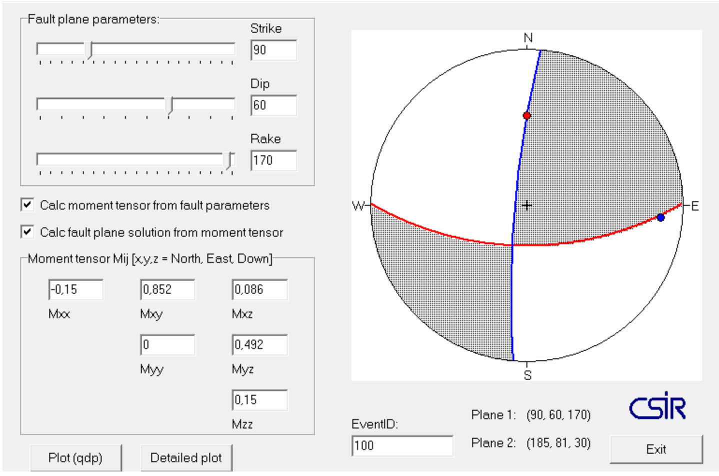

Fig. 6. Version of focal mechanism for the earthquake that occurred on 2019/05/16 in the Idaho region (t_0 = 09:08:57.00 (UTC), h_s = 6.91 km, φ = 44.578˚N, λ = –114.298˚E, ML = 2.4 – corresponding to components of seismic tensor obtained by the proposed inversion of waveforms at stations: HLID (42.56N, –114.41E) and MFID (43.42N, –115.83E) (see Fig. 5)

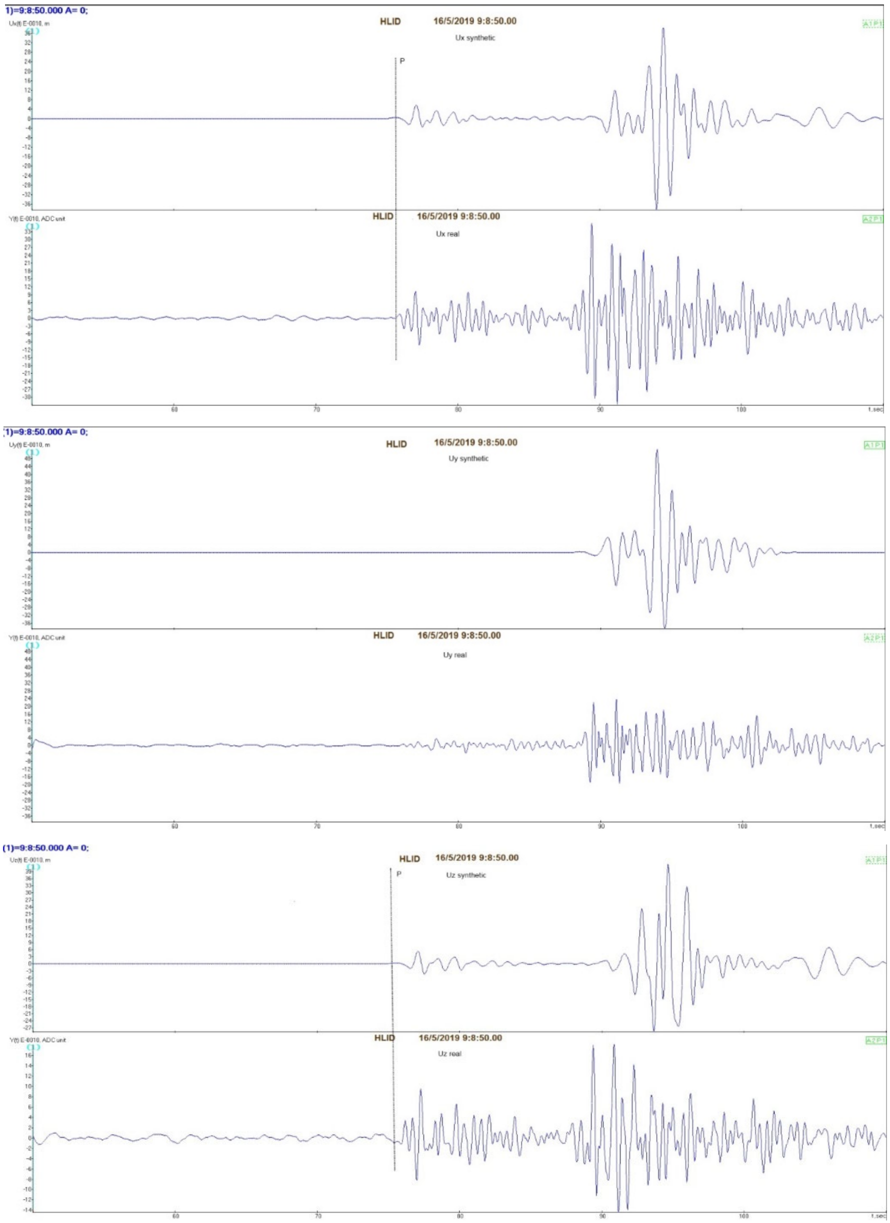

a

b

c

Fig. 7. Displacement seismograms at the station HLID (a – displacement at x-component; b – displacement at y-component; c-displacement at z-component) calculated by matrix method using the moment tensor *M(t)* determined for the earthquake of 2019/05/16 (Fig. 6) and the 1D crustal model listed in Table 1 (upper graphics) and the seismograms observed at the station (down graphics). Markers show the arrive of P-wave. The seismograms are filtered in the range 0.5–2.0 Hz

Discussion. In the paper, a possibility is explored of retrieving the components of seismic moment tensor from only direct P-wave forms at single station or at several stations. It is theoretically shown that the displacements at every single point on the upper surface of horizontally layered and perfectly elastic half-space generated by the point source represented by time-varying symmetric moment tensor depend on all of its six components, which can therefore be retrieved by inverting the dependence. Choosing to invert only the direct P-waves, calculated by matrix method, instead of the full field, enables to reduce the effects of the half-space model inaccuracy, reflected and converted phases being much more distorted by it.

The assumption of horizontally layered half-space, as well as the distribution of seismic velocities in it, may however turn out grossly incorrect in fact. Combined with inaccurate knowledge of source location and origin time, as well as with a number of the other uncertainties, such as introduced by seismic noise in the observed seismograms etc., it may almost completely obscure the source imprint in the seismograms, and especially in those originating, as it is, from only one station, turn the moment inversion ill-defined and lead to an intractable solution. That is why some independent means of control are needed for the results of any single station (and/or limited number of stations) inversion.

With this aim, we first propose to compare the mechanisms independently determined for the same earthquake from its waveforms at different single stations. For the earthquake of 2017/09/02 (event 1) they turn out almost indistinguishable between the stations AHID and (AHID and IMW) (Fig. 4), which at least means that despite all the uncertainties the unique solution exists and is reproducible. Next, synthetic waveforms at the stations HLID are calculated using the mechanism determined for the earthquake of 2019/05/16 (event 2) and compared with the waveforms observed at the station, the synthetics and observables appearing to correlate well in horizontal component *Ux* and in vertical *Uz* although slightly less in horizontal component *Uy* (Fig. 7). Finally, focal mechanism solutions for the earthquake of 2017/09/02 determined here by inversion of waveforms (Fig. 4, b, c) are compared from https://earthquake.usgs.gov/earthquakes/eventpage/us2000aekg/executive (Fig. 4, a).

Conclusions. In the paper, a method is presented for moment tensor inversion of only direct P-waveforms registered at only one station and a limited number of stations. The method is based on an inversion approach described in (*Malytskyy 2010, 2016*) where a version of the matrix method has been developed for calculation of direct P-waves in horizontally layered half-space from a point source represented by its moment tensor. Using the method presented in the current paper, focal mechanisms of the two earthquakes from the Idaho region of USA are retrieved. The mechanisms independently determined for the same earthquake from its waveforms at different single stations turned out almost identical (event 1). A conclusion is drawn out that the method will be useful when focal mechanisms cannot be obtained by other methods, the problem typical for the regions with low seismicity and insufficient number of seismic stations.

References

Aki, K., Richards, P.G. (1980). Quantitative Seismology: Theory and Methods. Vol. I. San Francisco: W.H. Freeman.

Arvidsson, R. (1996). Fennoscandian earthquakes: Whole crustal rupturing related to postglacial rebound. *Science,* 274, 744–746.

Arvidsson, R., Kulhanek, O. (1994). Seismodynamics of Sweden deduced from earthquake focal mechanisms, *Geophys. J. Int.*, 116, 377–392.

Camelbeeck, T., Iranga, M.D. (1996). Deep crustal earthquakes and active faults along the Rukwa trough, eastern Africa. *Geophys. J. Int.*, 124, 612–630.

Langston, C.A., Helmberger, D.V. (1975). A procedure for modelling shallow dislocation sources. *Geophys. J. R. astr. Soc.*, 42, 117–130.

Dziewonski, A., Woodhouse, J. (1983). An experiment in the systematic study of global seismicity: Centroid moment tensor solutions for 201 moderate and large earthquakes of 1981. *J. geophys. Res.,* 88, 3247–3271.

Fan, G., Wallace, T. (1991). The determination of source parameters for small earthquakes from a single, very broadband seismic station. *Geophys. Res. Lett.*, 18, 1385–1388.

Ferdinand, R.W, Arvidsson, R. (2002). The determination of source mechanisms of small earthquakes and revised models of local crustal structure by moment tensor inversion. *Geophys. J. Int.,* 151, 221–234.

Gilbert, F. (1970). Excitation of the normal modes of the Earth by earthquake sources. *Geophys. J. R. astr. Soc.*, 22, 223–226.

Given, J., Wallace, T., Kanamori, H. (1982). Teleseismic analysis of the 1980 Mammoth Lakes earthquake sequence. *Bull. seism. Soc. Am.*, 72, 1093–1109.

Godano, M., Bardainne, T., Regnier, M., Deschamps, A. (2011). Moment tensor determination by nonlinear inversion of amplitudes. *Bull.seism. Soc.Am.,* 101, 366–378.

Hardebeck, J.L., Shearer, P.M. (2003). Using S/P amplitude ratios to constrain the focal mechanisms of small earthquakes. *Bull.seism. Soc.Am.,* 93, 2432–2444.

Jost, M.L., Herrmann, R.B. (1989). A student's guide and review of moment tensors. *Seism. Res. Lett.*, 60, 37–57.

Kim, W.-Y. (1987). Modelling short-period crustal phases at regional distances for the seismic source parameter inversion. *Phys. Earth planet. Inter.*, 47, 159–177.

Koch, K. (1991, a). Moment tensor inversion of local earthquake data–I. Investigation of the method and its numerical stability with model calculations. *Geophys. J. Int.,* 106, 305–319.

Lay, T., Wallace, T. (1995). Modern Global Seismology. International Geophysics Series 58. San Diego: Academic Press.

Mai M., Schorlemmer D., Page M. et al. (2016). The Earthquake-Source Inversion Validation (SIV) Project. *Seism. Res. Lett.,* 87, 690–708. doi: 10.1785/0220150231.

Malytskyy, D. (2016). Mathematical modeling in the problems of seismology. Kyiv: Naukova Dumka. [in Ukrainian]

Malytskyy D. (2010). Analytic-numerical approaches to the calculation of seismic moment tensor as a function of time. *Geoinformatika,* 1, 79–85. [in Ukrainian]

Malytskyy, D., Kozlovskyy, E. (2014). Seismic waves in layered media, *J. of Earth Science and Engineering*, 4, 311–325.

Malytskyy, D., D'Amico, S. (2015). Moment tensor solutions through waveforms inversion. ISBN: 978-88-98161-13-3. Mistral Service S.a.S., Earth and Enviromental Sciences.

Mao, W.J., Panza, G.F., Sulhadolc, P. (1994). Linearized waveform inversion of local and near-regional events for source mechanism and rupturing processes. *Geophys. J. Int.*, 116, 784–798.

Nabelek, J.L. (1984). Determination of earthquake source parameters from inversion of body waves. *PhD thesis*. Massachusetts Institute of Technology, Cambridge.

Nabelek, J., Xia, G. (1995). Moment-tensor analysis using regional data: application to the 25 March, 1993, Scotts Mills, Oregon, earthquake. *J. geophys. Res*., 22, 13–16.

Pang, G, Koper, K.D., Stickney, M.C. et al. (2018). Seismicity in the Challis, Idaho, Region, January 2014–May 2017: Late Aftershocks of the 1983 Ms 7.3 Borah Peak Earthquake. *Seism. Res. Lett.*, 89, 1366–1378.

Saikia, C.K., Herrmann, R.B. (1985). Application of waveform modeling to determine focal mechanisms of four 1982 Miramichi aftershocks. *Bull. seism. Soc. Am.,* 75, 1021-1040.

Shemeta, J.E. (1989). New analyses of three-component digital data for aftershocks of the 1983 Borah Peak, Idaho, earthquake: Source parameters and refined hypocenters. *M.S. Thesis.* Department of Geology and Geophysics, University of Utah.

Shomali, Z.H., Slunga, R. (2000). Body wave moment tensor inversion of local earthquakes: an application to the South Iceland seismic zone. *Geophys. J. Int.,* 140, 63–70.

Sileny, J., Psencik, I. (1995). Mechanisms of local earthquakes in 3D inhomogeneous media determined by waveform inversion. *Geophys. J. Int.,* 121, 459–474.

Sileny, J., Panza, G.F., Campus, P. (1992). Waveform inversion for point source moment tensor retrieval with variable hypocentral depth and structural model. *Geophys. J. Int.,* 109, 259-274.

Sileny, J., Campus, P., Panza, G.F. (1996). Seismic moment tensor resolution by waveform inversion of a few local noisy records–I. Synthetic tests. *Geophys. J. Int.,* 126, 605–619.

Singh, S.K., Ordaz, M., Pacheco, J.F., Courboulex, F. (2000). A simple source inversion scheme for displacement seismograms recorded at short distances. *J. Seism.,* 4, 267–284.

Sipkin, S.A. (1986). Estimation of earthquake source parameters by the inversion of waveform data, global seismicity 1981–1983. *Bull. seism. Soc. Am.,* 76, 1515–1541.

Stump, B.W., Johnson, L.R. (1977). The determination of source properties by the linear inversion of seismograms. *Bull. seism. Soc. Am.*, 67, 1489–1501.

Vavrychuk V., Kuhn D. (2012). Moment tensor inversion of waveforms: a two-step time frequency approach. *Geophys. J. Int.,* 190, 1761–1776.

Weber, Z. (2016). Probabilistic waveform inversion for 22 earthquake moment tensors in Hungary: new constraints on the tectonic stress pattern inside the Pannonian basin. *Geophys. J. Int.,* 204, 236–249.

Weber, Z. (2006). Probabilistic local waveform inversion for moment tensor and hypocentral location. *Geophys. J. Int.,* 165, 607–621.

Zhao, L-S., Helmberger, D.V. (1994). Source estimation from broadband regional seismograms. *Bull. seism. Soc. Am.*, 84, 91–104.

Zhu, L., Helmberger, D.V. (1996). Advancement in source estimation techniques using broadband regional seismograms. *Bull. seism. Soc. Am.*, 86, 1634–1641.

Надійшла до редколегії 28.08.2020

Д. Малицький[1], д-р фіз.-мат. наук, проф.,
E-mail: dmalytskyy@gmail.com;
Д. Майксел[1,2], PhD, проф.,
E-mail: DylanMikesell@boisestate.edu;
[1]Карпатське відділення Інституту геофізики ім. С.І. Субботіна НАН України,
вул. Наукова, 3, б, м. Львів, 79060, Україна;
[2]Відділення наук про Землю, Університет м. Бойзе,
1910 Юніверсіті Драйв, Бойзе, Айдахо, 83725 США

ВИЗНАЧЕННЯ ФОКАЛЬНИХ МЕХАНІЗМІВ МАЛИХ ЗЕМЛЕТРУСІВ ШЛЯХОМ ОБЕРНЕННЯ ЇХНІХ ХВИЛЬОВИХ ФОРМ

Представлено метод для визначення тензора сейсмічного моменту з використанням тільки прямих Р-хвиль, які реєструються на одній і на обмеженій кількості станцій. Метод базується на роботах авторів, у яких розвинута версія матричного методу для обчислення поля переміщень тільки для прямих Р-хвиль, які поширюються в горизонтально-шаруватому півпросторі від точкового джерела, що представлено тензором сейсмічного моменту. Ми описуємо процедуру визначення фокального механізму малих землетрусів і показуємо її застосування на прикладі двох місцевих землетрусів, які відбулися в регіоні м. Бойзе (США). Визначення тензора сейсмічного моменту шляхом обертання їхніх хвильових форм базується на точковій моделі джерела, а також на методі для визначення синтетичних сейсмограм за допомогою матричного методу для хвиль, які поширюються в пружному, горизонтально-шаруватому середовищі. У роботі показано, що обернення лише прямих Р-хвиль дозволяє зменшити вплив неточності моделі середовища, оскільки прямі хвилі зазнають набагато меншого спотворення через неточність, аніж відбиті й конвертовані. Цей підхід значно поліпшує точність і надійність методу обернення хвильових форм для визначення фокального механізму. Вогнище землетрусу розглядається як точкове із заздалегідь відомим розташуванням і часом виникнення. На основі розв'язку прямої задачі й з використанням т. зв. розв'язку узагальненого обернення розроблено алгоритм обернення спостережуваних хвильових форм з метою визначення компонент сейсмічного тензора M(t).

Ключові слова: тензор сейсмічного моменту, фокальний механізм, малі землетруси, матричний метод.

Д. Малицкий[1], д-р физ.-мат. наук, проф.,
E-mail: dmalytskyy@gmail.com;
Д. Майксел[1,2], PhD, проф.,
E-mail: DylanMikesell@boisestate.edu;
[1]Карпатское отделение Института геофизики им. С.И. Субботина НАН Украины,
ул. Научная, 3, б, г. Львов, 79060, Украина;
[2]Отделение наук о Земле, Университет г. Бойзэ,
1910 Юниверсити Драйв, Бойзє, Айдахо, 83725 США

ОПРЕДЕЛЕНИЕ ФОКАЛЬНЫХ МЕХАНИЗМОВ МАЛЫХ ЗЕМЛЕТРЯСЕНИЙ ПУТЕМ ОБРАЩЕНИЯ ИХ ВОЛНОВЫХ ФОРМ

Представлен метод для определения тензора сейсмического момента с использованием только прямых Р-волн, регистрируемых на одной и на ограниченном количестве станций. Метод основан на подходе, описанном в работах авторов, в которых развита версия матричного метода для вычисления поля перемещений только для прямых Р-волн, которые распространяются в горизонтально-слоистом полупространстве от точечного источника, представленного тензором сейсмического момента. Мы описываем процедуру определения фокального механизма малых землетрясений и показываем ее применение на примере двух местных землетрясений, которые произошли в регионе г. Бойзэ (США). Определение тензора сейсмического момента путем обращения их волновых форм базируется на точечной модели источника, а также на методе для определения синтетических сейсмограмм с помощью матричного метода для волн, распространяющихся в упругой, горизонтально-слоистой среде. В работе показано, что обращение только прямых Р-волн позволяет уменьшить влияние неточности модели среды, поскольку прямые волны испытывают гораздо меньшие искажения, чем отраженные и конвертируемые. Этот подход значительно улучшает точность и надежность метода обращения волновых форм для определения фокального механизма. Очаг землетрясения рассматривается как точечный, с известным расположением и времени возникновения. На основе решения прямой задачи и с использованием обобщенного обращения разработан алгоритм обращения наблюдений волновых форм с целью определения компонент сейсмического тензора M (t).

Ключевые слова: тензор сейсмического момента, фокальный механизм, малые землетрясения, матричный метод.